Biomedicine & Pharmacotherapy 127 (2020) 110155

Contents lists available at ScienceDirect

Biomedicine & Pharmacotherapy

journal homepage: www.elsevier.com/locate/biopha

Dehydroabietic acid alleviates high fat diet-induced insulin resistance and hepatic steatosis through dual activation of PPAR-γ and PPAR-α

Zhishen Xie[a], Gai Gao[a], Hui Wang[a], Erwen Li[a], Yong Yuan[a], Jiangyan Xu[a,*], Zhenqiang Zhang[a,*], Pan Wang[a], Yu Fu[a], Huahui Zeng[a], Junying Song[a], Christian Hölscher[a], Hui Chen[b]

[a] Academy of Chinese Medical Sciences, Henan University of Chinese Medicine, Zhengzhou, 450046, China
[b] School of Life Sciences, Faculty of Science, University of Technology Sydney, PO Box 123, Broadway, NSW, 2007, Australia

ARTICLE INFO

Keywords:
Dehydroabietic acid
Insulin resistance
Hepatic steatosis
Hyperlipidemia
PPARs

ABSTRACT

Dual-PPAR-α/γ agonist has the dual potentials to improve insulin resistance (IR) and hepatic steatosis associated with obesity. This study aimed to investigate whether dehydroabietic acid (DA), a naturally occurred compound, can bind to and activate both PPAR-γ and PPAR-α to ameliorate IR and hepatic steatosis in high-fat diet (HFD)-fed mice.. We found that DA formed stable hydrogen bonds with the ligand-binding domains of PPAR-γ and PPAR-α. DA treatment also promoted 3T3-L1 differentiation *via* PPAR-γ activation, and mitochondrial oxygen consumption in HL7702 cells *via* PPAR-α activation. In HFD-fed mice, DA treatment alleviated glucose intolerance and IR, and reduced hepatic steatosis, liver injury markers (ALT, AST), and lipid accumulation, and promoted mRNA expression of PPAR-γ and PPAR-α signaling elements involved in IR and lipid metabolism in *vivo* and *in vitro*, and inhibited mRNA expression of pro-inflammatory factors. Therefore, DA is a dual-PPAR-α/γ and PPAR-γ partial agonist, which can attenuate IR and hepatic steatosis induced by HFD-consumption in mice.

1. Introduction

Diabetes mellitus (DM) is a global disease [1,2], 1 in 10 people are living with diabetes, according to the international diabetes federation's report. Insulin resistance (IR) is the major feature of type 2 diabetes (T2DM), the most common type of diabetes, accounting for around 90 % of all DM cases. T2DM is a chronic metabolic disease, usually associated with obesity, hyperlipidemia, hepatic steatosis, *etc* [3–5].

Peroxisome proliferator-activated receptor (PPAR)-α and PPAR-γ belong to the nuclear receptor superfamily [6,7]. PPAR-γ regulates adipogenesis and insulin sensitivity [8], whose selective agonists (thiazolidinediones (TZDs), such as thiazolidinediones and rosiglitazone (RSG)) have been used as 2nd line anti-type 2 diabetic drugs for decades. These two drugs clinically used as PPAR-γ agonists can remodel adipose tissue resulting in adipocyte hypertrophy and hyperplasia, which is used as a mechanism to improve systemic insulin sensitivity [9,10]. On the other hand, such newly differentiated adipocytes are insulin sensitive which facilitates postprandial glucose uptake and conversion into triglycerides (TG) for long-term storage. As such, weight gain is a significant side effect of thiazolidinediones and RSG, in addition to liver toxicity which requires regular surveillance of liver function. Troglitazone, strongly activates PPAR-γ, has been discontinued in clinical use, because of undesirable clinical side effects such as weight gain, liver damage and osteoporosis [11]. PPARα is widely expressed and serves to activate FAO pathways in many tissues and cells including the intestine, vascular endothelium, smooth muscle and immune cells such as monocytes, macrophages and lymphocytes and the liver controls several key genes [12], involved in lipid homeostasis [13,14], including lipolysis and mitochondrial fatty acid β-oxidation [15,16], permit efficient use of mobilized lipids and decrease secretion of triglycerides (TGs) from the liver and promote TG clearance from plasma, and thereby also reduce atherogenic lipoprotein particles. It was this activity that prompted therapeutic development to reduce cardiovascular risk, fat liver in patients with raised plasma lipids [13].. Metabolic disorders such as diabetes, atherosclerosis, hyperlipidemia and obesity, rarely occur in isolation, but usually arise in the same individuals. Large numerous studies have shown that the development of PPAR-α/γ dual agonists or PPAR-γ partial agonists are developed to increase insulin sensitivity and alleviate hepatic steatosis is a promising approach [17–19].

Dehydroabietic acid (DA), is a derivative of abietic acid (AA) which is the primary irritant in pinewood [20]. DA and AA also derive from rosin, which is often used for plucking duck feather. Therefore, DA was found in raw and cooked ducks [21].DA and AA have been shown to

* Corresponding authors.
E-mail addresses: xujiangyan2008@163.com (J. Xu), zhang_zhenqiang@126.com (Z. Zhang).

https://doi.org/10.1016/j.biopha.2020.110155
Received 5 March 2020; Received in revised form 1 April 2020; Accepted 8 April 2020

have anti-aging [22], anti-inflammatory [23–25], anti-bacterial [26], and anti-cancer effects [27,28]. In the genetic obese diabetic KK-Ay mice, DA supplement in the chow has been shown to effectively reduce fasting blood glucose levels [29]. DA increased expression of PPAR-γ and-α [23] and stimulated insulin dependent glucose uptake into 3T3-L1 adipocyte in *vitro* [30]. It is reasonable to assume that DA may overcome such side effects of TZDs due to it proposes dual PPAR-γ/α action. In addition, the anti-inflammatory effects *via* inhibiting NF-κB signaling pathway elements are commonly proposed mechanisms in improving systemic insulin sensitivity, as inflammation plays a key role in compromising insulin signaling cascade [24,29], in addition to increasing adiponectin and glucose uptake by Glut-4 [29]. It was also shown that the DA treatment suppressed the production of monocyte chemoattractant protein-1 (MCP-1) and tumor necrosis factor-α (TNF-α) (proinflammatory cytokines) [29], inhibited NF-κB signaling pathway [24], increased adiponectin expression (an anti-inflammatory cytokine) [29]. Both in *vitro* and in *vivo* studies identified PPAR-γ/α influences on both acute and chronic inflammatory processes [13,31]. Taken together, it is reasonable to assume that DA could alleviate IR and hepatic steatosis *via* activate PPAR-γ/α and overcome such side effects of TZDs.

In this study, we found that DA is a dual-PPAR-α/γ and PPAR-γ partial agonist and firstly provided visual evidence of how DA and AA bind to PPAR-γ and PPAR-α. The effects on metabolic phenotypes of IR and hepatic steatosis were verified in high fat diet (HFD)-induced obese mice, an animal model more consistent with human diabetes mellitus. DA promotes fatty acid β-oxidation, prevents IR and hepatic steatosis which maybe depend on PPAR-γ and PPAR-α activation. As expected, DA overcome PPAR-γ side effects such as weight gain and fat liver.

2. Materials and methods

2.1. Reagents

Dulbecco's modified Eagle's medium (DMEM, Gibco, US); Fetal bovine serum (FBS; Gibco, US); Penicillin-streptomycin solution (Solarbio, China); HEK293 T, 3T3-L1 and HL7702 cell (ATCC, US); Dehydroabietic acid (DA), abietic acid (AA), Rosiglitazone (RSG); Oleic acid, Dexamethasone (Dex), Oil red O, GW9662 (Aladdin, China); Insulin (Ins, MedChemExpress, US); WY14643 (Selleck Chemicals, US); GW6471 (Glpbio, US); Nile red (Macklin, China), 3-(4,5-dimethyl-2-thiazolyl)-2,5-diphenyl-2-H-tetrazolium bromide (MTT, Solarbio, China); Sodium carboxymethylcellulose, Dimethyl sulfoxide (DMSO, Macklin, China); D12492 (Jiangsu Xietong Pharmaceutical Bio-engineering Co., Ltd., China).

2.2. PPAR-γ and PPAR-α binding assays

For the PPAR-γ or PPAR-γ -α activity assay, plasmid pSG5-PPAR-γ or PPAR-γ -α and the PPAR promoter–reporter vector J3-TKLuc were used as previously described [32]. For PPAR-γ-LBD or PPAR-α-LBD assay, plasmid GAL4-PPARγ-LBD or GAL4-PPAR-α-LBD fusion protein and a pGL4.35 reporter were used [33].

HEK293 T cells were seeded at a density of 2×10^4 cells per well into 96-well plates for 18 h and transfected over a 6 h period with 100 ng plasmid expressed target genes and 10 ng of β-galactosidase reporter to normalize transfection efficiencies using lip2000 transfection reagents. Then, they were treated with DA or AA (2.5–50 μM) or RSG (0.0001–50 μM) for 24 h. The luciferase was detected using the luciferase reporter assay kit (Promega, US).

2.3. Cell culture

Pre-adipocyte 3T3-L1 and human liver cell HL7702 were maintained in DMEM high glucose medium containing 10 % FBS and 1% penicillin-streptomycin solution and cultured at 37 °C in 5% CO_2 incubator (Thermofisher). Cell viability was tested in 3T3-L1 and HL7702 cells with various doses of DA and AA using MTT assay.

For 3T3-L1 cell differentiation, cells were seeded into 6-well plates to full confluence for 2 days, and then induced by completed medium containing 10 μg/mL insulin, 1 μM dexamethasone. After 2 days of induction, the medium was replaced with a maintenance medium (completed medium including 10 μg/mL insulin) as well as different compounds (20 μM RSG, or 2.5, 5, 10, 15 μM DA) The last incubation lasted for 4 days before Oil Red O staining as previously reported [34]. For quantification, oil red O was extracted by isopropanol for 20 min. at room temperature and then transferred it to a 96-well plate, and measured the absorbance value at 500 nm.

To investigate the effects on the expression of PPAR-γ target genes, 3T3-L1 cells were collected at 0th, 4th and 6th day during the differentiation with test compound for *Glut-4*, *Cyp4a10* and *Scd-1* mRNA measurement.

2.4. Intracellular lipid analysis and oxygen consumption of HL7702 cells

For intracellular lipid analysis, HL7702 cells were plated at 2×10^5 cells per well in 6-well plates and treated with different compounds (10 μM WY14643 (PPAR-α agonist)), or 2.5, 5, 10 μM DA or 10 μM DA + 10 μM GW6471 (PPARα antagonist) together with 0.6 mM oleic acid for 24 h. The cells were stained with nile red and observed by fluorescence microscopy and lipid drops observed by transmission electron microscope (JEM-1400; JEOL Ltd., Tokyo, Japan) [35].

Oxygen consumption rate (OCR) was measured by Seahorse bioanalyzer as previously described. Briefly, HL7702 cells were seeded at a density of 2.5×10^4 cells per well in a collagen coated XFe96 cell culture microplate, with or without the test compounds (10 μM WY14643, or 2.5, 5, 10 μM DA or 10 μM DA + 10 μM GW6471) for 23 h prior to the assay. Oligomycin (1 μM), FCCP (1 μM) and Rotenone and Antimycin A (1 μM) were administered during the assay according to manufacturer's instructions.

2.5. Animal experiments

All animal protocols were approved by the State of Animal Ethics Committee of Henan University of Chinese Medicine (DWLL201912032). The mice were kept with constant temperature (22 ± 2 °C) and humidity (55 %) with a 12 h light/dark cycle with water and food *ad libitum*. After one week of adaptation to the environment, male C57BL/6 J mice (8 weeks, Beijing Vital River Laboratory Animal Technology Co., Ltd., China) were fed normal chow diet (NCD, 10 % energy from fat) and high-fat diet (HFD, 60 % energy from fat, 20 % energy from protein, Cat. D12492, Jiangsu Xietong Pharmaceutical Bio-engineering Co., Ltd., China) for 12 weeks [36]. Then, the HFD mice were randomly divided into 4 groups and gavaged with rosiglitazone (RSG, 4 mg/kg/d), low dose of DA (DA-L, 10 mg/kg/d), high dose of DA (DA-H, 20 mg/kg/d) [29], and saline respectively for 9 weeks (n = 8–12). NCD group received 0.5 % CMC-Na.

After 7 weeks of treatment, an insulin tolerance test (ITT) was performed following 6 h fasting. After insulin injection (1 IU/kg, *i.p.*), blood was taken from the tail vein at 0, 30, 60, 90, 120, 150 min. After 4 days, oral glucose tolerance test (OGTT) was carried out following 12 h fasting. After glucose administration (2 g/kg, gavage), blood was taken from the tail vein at 0, 15, 30, 60, 90, 120 min post gavage. The area under the curve (AUC) was calculated for each mouse (GraphPad Prism 7.0).

At the endpoint, liver, interscapular brown fat, and epididymal fat pads were fixed in 4% paraformaldehyde for immunohistochemistry staining as previously described [37], or snap frozen in liquid nitrogen and store at −80 °C for mRNA measurement.

2.6. Bioassays

Plasma aspartate aminotransferase (AST), alanine aminotransferase (ALT), triglyceride (TG), total cholesterol (TC), low-density lipoprotein cholesterol (LDL-c) and high-density lipoprotein cholesterol (HDL-c) were measured in the blood by the automatic biochemical analyzer (OLYMPUS AU400, Japan).

2.7. Histological and immunohistochemical analysis

Fresh liver and fat sections were fixed with 4% paraformaldehyde, embedded in paraffin, and cut into 4 μm sections for hematoxylin-eosin (H&E) staining. Images were obtained with an Olympus microscope-camera system (Tokyo, Japan). Adipocyte cell size was measured in H&E stained tissues [38] and quantified by Image J software (Image J, National Institutes of Health, MD, USA). Immunohistochemical staining was performed using monoclonal anti-PPAR-α (1 : 200, Servicebio), ati-ACADM antibody (1 : 200, Servicebio), mouse anti-UCP-1 (1 : 200, ABclonal) and anti-CPT1α (1 : 200, ABclonal) as previously published [37,39] and quantification by ImageJ (Media Cybernetics, Inc, USA). Clinical nonalcoholic steatohepatitis (NASH) Activity Score (NAS) was used to assess the liver as previously described [40].

2.8. Quantitative real-time PCR

Total RNAs were isolated using trizol (Vazyme, China). Equal amounts of RNA from 8 mice were pooled [41,42] for cDNA synthesis using a cDNA synthesis kit (Beyotime, China). Quantitative real-time PCR was performed using SYBR green primers (sequences in Supplementary Table 1, ABI 7500), GAPDH was used as a housekeeping gene, and the expression of the target genes was calculated according to the formula $2^{-\triangle\triangle Ct}$.

2.9. Statistical analysis

Data were expressed as the mean ± standard error of the mean (SEM). Comparisons between two groups were assessed using Student's t-test, and comparisons for more than 2 groups were analyzed using one-way analysis of variance (ANOVA) followed by Dunnett's post hoc tests (GraphPad Prism 7.0). $p < 0.05$ was considered statistically significant.

3. Results

3.1. DA is a dual-PPAR-α/γ and PPAR-γ partial agonist

Firstly, we investigated the effect of DA on the activity of PPAR-γ and PPAR-α. As shown in Fig. 1A, DA induced more than 3 times activation of PPAR-γ compared with AA, however only to ¼ of which RSG has achieved at the same dose. DA also induced ~5 times the activity of PPAR-γ (LBD) than that of AA (Fig. 1B). Molecular docking results suggest that DA and AA binding to the LBD of PPAR-γ at ARG280 by forming 3 and 2 hydrogen bonds, respectively. DA showed lower binding energy than AA (Fig. 1C, D). More importantly, DA also induced 1.4 times more activities of PPAR-α than AA (Fig. 1E). The PPAR-α-LBD activation was also ~1.8 times higher with DA than AA (Fig. 1F). DA formed hydrogen bonds with PPAR-α-LBD at ARG465 and LYS448, while AA at LYS448 and LYS449. DA also had lower binding energy with PPAR-α-LBD than AA (Fig. 1G, H) Taken together, DA is a natural PPAR-γ partial agonist and also a dua-PPAR-α/γ agonist.

3.2. DA promotes pre-adipocytes differentiation and PPAR-γ activities in adipocytes

In liver cells line HL7702 and pre-adipocytes 3T3-L1, DA treatment (100 μM) only marginally decreased cell viability, and DA showed less toxicity than AA (Supl Fig S1A and B). Therefore, DA was used for the rest *in vitro* and in *vivo studies*.

Promoting pre-adipocytes differentiation is an important mechanism for how RSG improves glycemic control. We compared the effects of DA and RSG on pre-adipocyte 3T3-L1 differentiation. As shown in Fig. 2A, DA promoted 3T3-L1 adipocyte differentiation in a dose-dependent manner. Oil red O staining also showed a dose-dependent effect of DA to increase lipid deposition in the adipocytes with the strongest effect at 15 μM ($F(5, 42) = 388.6$, $p < 0.001$, Fig. 2B). However, 10 μM was chosen for later *in vitro* studies based on the cell viability assays (Supl Fig. S1).

mRNA expression of PPAR-γ target genes involved in pre-adipocytes differentiation *Glut-4*, *Scd-1* and *Cyp4a10*, showed a time-dependent increase during the differentiation. DA exerted similar effect as RSG to increase *Glut-4* (Fig. 2C) and *Cyp4a10* expression (Fig. 2D), however less effect than RSG on *Scd-1* ($F(2, 6) = 16.92$, $p = 0.0034$, Fig. 2E) on day 6 of the differentiation.

In differentiated adipocytes, DA at 10 μM exerted similar effects as RSG at 20 μM to upregulate mRNA expression of known PPAR-γ target genes, including those involved in adipogenesis (CAAT/enhancer binding protein β (*CEBPB*), fatty acid binding protein 4 (*FABP4*), cortisone reductase 11β-hydroxysteroid dehydrogenase 1 (*11β-HSD1*), mitochondrial carbohydrate metabolic marker Pyruvate Dehydrogenase Lipoamide Kinase Isozyme 4 (*PDK4*)), while the effect on the lipid metabolic regulator phosphodiesterase 3 (*PED3B*) was stronger than the RSG ($F(2, 6) = 31.59$, $p = 0.0007$, Fig. 3A). DA treatment increased transcription of the insulin sensing *adiponectin* ($F(2, 6) = 31.34$, $p = 0.0007$; $p < 0.001$ *vs.* DMSO, Fig. 3B), and lipid metabolic marker angiopoietin-like protein 4 (*ANGPTL4*, $F(2, 6) = 114.6$, $p < 0.0001$, Fig. 3C), at much higher levels than RSG treatment ($p < 0.001$, DA10 *vs.* RSG). Furthermore, DA had similar effect to RSG to increase the mRNA expression of *leptin* ($F(2, 6) = 7.806$, $p = 0.0214$, Fig. 3D) and the regulator of lipid and glucose metabolism, fibroblast growth factor 21 (*FGF21*, $F(2, 6) = 162.8$, $p < 0.0001$, Fig. 3E), and reduce the mRNA expression of inflammatory regulator angiopoietin-like protein 2 (*ANGPTL2*, $F(2, 6) = 31.51$, $p = 0.0007$, Fig. 3F) and retinoic acid receptor responder 2 (*PARRES2*, $F(2, 6) = 5.86$, $p = 0.0388$, Fig. 3G) which encodes the adipokine Chemerin involved in adipocyte differentiation and lipolysis.

3.3. DA decreases lipid accumulation and promotes mitochondrial function via PPAR-α in HL7702 cells

Oleic acid was used to induce lipid accumulation in HL7702 cells. Nile red binds to lipids and gives off orange fluorescence, which is often used to analyze cell lipid contents. As expected, oleic acid increased lipid accumulation in the HL7702 cells, which was prevented by both DA and PPAR-α agonist WY14643 (Fig. 4A, C; $F(4, 25) = 22.93$, $p < 0.0001$; both $p < 0.001$ *vs.* Oleic acid). However, GW6471, a selective PPAR-α antagonist, blocked the effect of DA on Oleic acid – induced lipid accumulation, which suggested this effect of DA is PPAR-α mediated (Fig. 4A, C). This was further confirmed by the measurement of the areas of the lipid droplets by electron microscope ($F(4, 25) = 36.97$; $p < 0.0001$, Fig. 4B, D).

Using a seahorse assay, mitochondrial oxygen consumption rates (OCR) were measured in HL7702 cells. WY14643 had the strongest effect to enhance mitochondrial activities including ATP synthesis, followed by DA (Fig. 4E, F). However, GW6471 only partially blocked this effect of DA, suggesting DA also works on other pathways to regulate mitochondrial metabolism (Fig. 4E, F). As shown in Fig. 4G, DA upregulated the expression of classical PPAR-α target genes mostly at 10 μM, including those genes involved in fatty acid β-oxidation (carnitine palmitoyl transferase 1α (*CPT-1α*, $F(3, 8) = 81.52$, $p < 0.0001$), acyl-CoA dehydrogenase, long chain (*ACDAL*, $F(3, 8) = 31.54$, $p < 0.0001$) and uncoupling protein-3 (*UCP-3*,$F(3, 8) = 71.75$, $p < 0.0001$). It needs to be noted that the effect of DA on gene

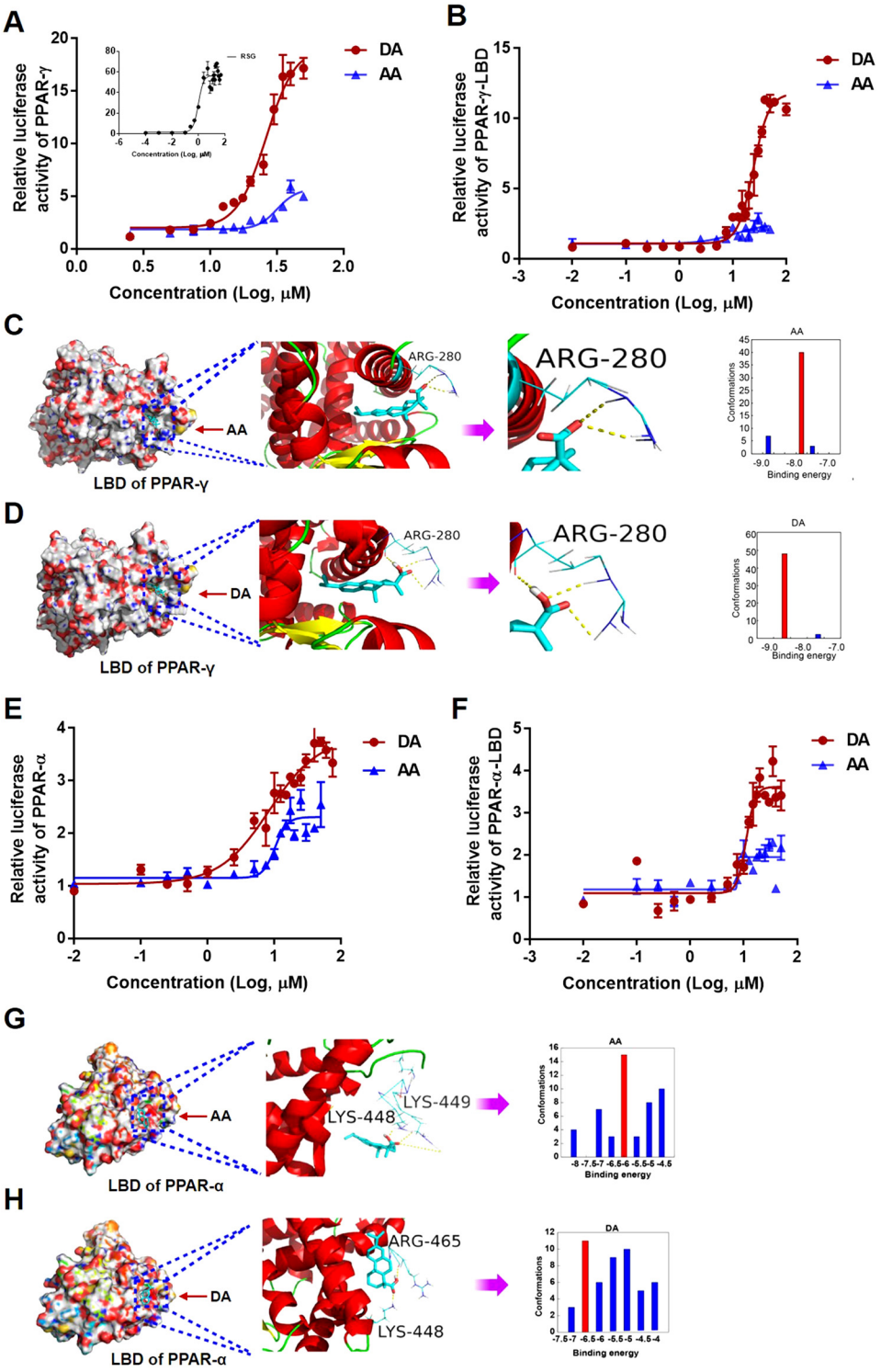

Fig. 1. DA is a dual-PPAR-α/γ and PPAR-γ partial agonist. (A) DA and AA activated PPAR-γ (n = 3). (B) DA and AA activated the LBD of PPAR-γ. (C) and (D) DA and AA docking with LBD of PPAR-γ (PDB: 6ENQ). (E) DA and AA activated PPAR-α (n = 3). (F) DA and AA activated the LBD of PPAR-α. (G) and (H) DA and AA docking with the LBD of PPAR-α (PDB ID: 2REW) DA: Dehydroabietic acid; AA: Abietic acid; LBD: Ligand-binding domains.

expression is not always comparable to PPAR-α agonist WY14643, stronger on some genes whereas weaker on the others than WY14643, suggesting that other pathways may be activated by DA.

3.4. DA alleviates HFD-induced glucose intolerance and insulin resistance in vivo

As shown in Fig. 5A ($F(4, 35) = 20.47$, $p < 0.0001$), after 21 weeks of HFD consumption, the HFD mice gained ~30 % more body weight compared to NCD mice ($p < 0.001$). However, RSG did not prevent further weight again in HFD-fed mice, whereas DA significantly

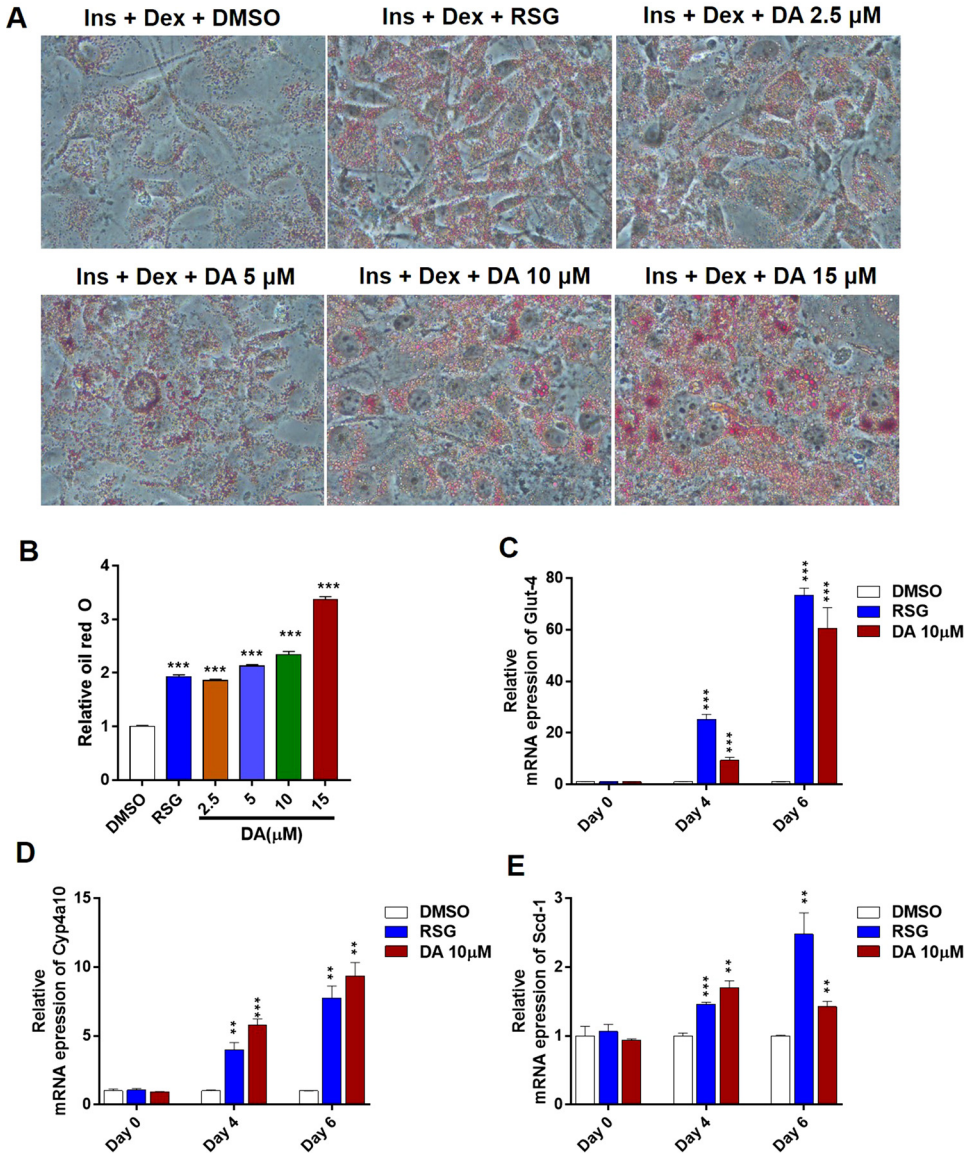

Fig. 2. DA promotes 3T3-L1 cells differentiation *in vitro*. (A) representative images of 3T3-L1 cells stained with Oil Red O on day 6 of differentiation. Ins + Dex, 10 μg/mL insulin + 1 μM dexamethasone. (B) Quantitative analysis of oil red O in adipocytes at 6th day of differentiation (n = 6). (C-E) Effect of DA on *Glut-4*, *Cyp4a10, Scd-1* mRNA expression during different days of 3T3-L1 differentiation (n = 3). $*p < 0.05$, $**p < 0.01$ and $***p < 0.001$ *vs.* DMSO at the same day. Data are expressed as mean ± SEM, DA: Dehydroabietic acid; AA: Abietic acid; Ins: insulin; Dex: Dexamethasone.

reduced the body weight of HFD-fed mice in a dose-dependent manner ($p < 0.05$ DA-L *vs.* HFD; $p < 0.001$ DA-H *vs.* HFD, Fig. 5A). Fasting blood glucose level was decreased in the HFD mice as expected ($p < 0.001$ *vs.* NCD, Fig. 5B), which was nearly normalized by RSG as expected (Fig. 5B; F (4, 35) = 10.61, $p < 0.0001$; $p < 0.01$ *vs.* HFD). DA-H had a similar hypoglycemia effect as RSG ($p < 0.01$ *vs.* HFD) but DA-L not ($p < 0.05$ *vs.* HFD). During OGTT, the effects of RSG and DA on blood glucose level mirrored fasting glucose level (Fig. 5C, D; F (4, 35) = 9.875, $p < 0.0001$). During ITT, both doses of DA showed similar effects as RSG to improve insulin sensitivity (Fig. 5E, F; F (4, 35) = 36.74, $p < 0.0001$).

Next, we identified whether DA improves IR is PPAR-γ dependent. As shown in Sup Fig S2A (F (3, 28) = 48.64, $p < 0.0001$), the level of fasted blood glucose was significantly reduced by DA treatment ($p < 0.0001$ *vs.* HFD), which was partially reversed by additional GW9662, a selective PPAR-γ antagonist ($p < 0.001$ DA + GW9962 *vs.* DA). During OGTT and ITT, the effect of DA on blood glucose levels was completely blocked by additional GW9962 (Sup Fig S2B, C, D and E; C: F (3, 20) = 84.91, $p < 0.0001$; E:F (3, 28) = 33.02, $p < 0.0001$). These data suggest that the effect of DA on glycemic control and insulin action is PPAR-γ dependent.

3.5. DA alleviates HFD-induced hepatic steatosis and inflammation in vivo

DA also improved hepatic steatosis and dyslipidemia *in vivo*. As shown in Fig. 6A–C, both gross anatomy and H&E staining showed severe ectopic fat deposition in the liver of HFD mice reflected by NAFLD score and ballooning (F (4, 35) = 18.4, $p < 0.0001$; $p < 0.001$ *vs.* NCD, Table 1), in addition to increasing inflammatory score (F (4, 35) = 15.15, $p < 0.0001$; $p < 0.001$ *vs.* NCD, Table 1), Compared with RSG, DA had a better effect to ameliorate hepatic steatosis related markers in a dose-dependent manner (Fig. 6A–C, Table 1; C: F (4, 35) = 70.91, $p < 0.0001$). As such, liver injury markers, ALT and AST were also nearly normalized by DA treatment regardless of the dose (both $p < 0.001$ *vs.* HFD, Fig. 6D, E; D: F (4, 40) = 15.9, $p < 0.0001$; E: F (4, 40) = 25.25, $p < 0.0001$); whereas both were further increased by RSG treatment ($p < 0.05$ *vs.* HFD, Fig. 6D, E) consistent with its side effects in diabetic patients. DA also significantly decreased blood TG, TC and

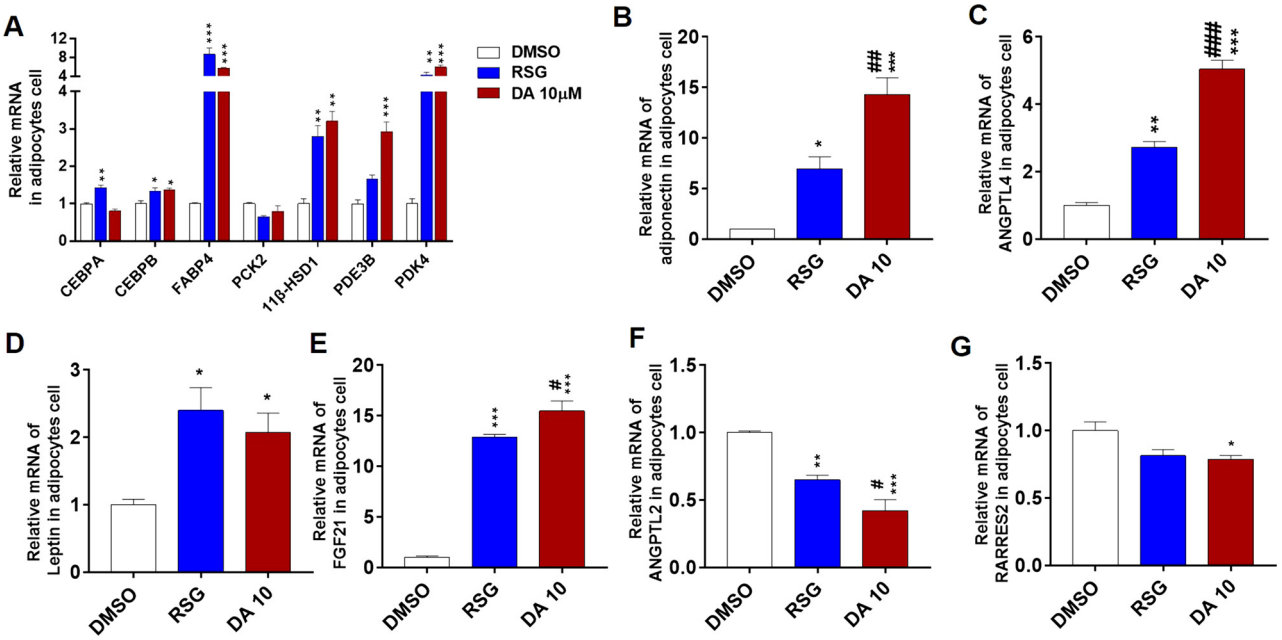

Fig. 3. DA selectively activates PPAR-γ in differentiated 3T3-L1 cells. mRNA expression of known PPAR-γ target genes (A) and *adiponectin* (B), *ANGPTL4* (C), *Leptin* (D), *FGF21* (E), *ANGPTL2* (F), *RARRES2* (G) in differentiated 3T3-L1 cells after treated with 10 μM RSG or 10 μM DA for 24 h. Data are expressed as mean ± SEM, n = 3, DA10: dehydroabietic acid 10 μM; RSG: rosiglitazone. $^{*}p < 0.05$, $^{**}p < 0.01$ and $^{***}p < 0.001$ *vs.* DMSO group; $^{\#}p < 0.05$, $^{\#\#}p < 0.01$ and $^{\#\#\#}p < 0.001$ DA 10 *vs.* RSG group.

LDL-c levels in the HFD mice, and increased their HDL-c levels (Table 2, F (4, 35) = 31.16, $p < 0.0001$), suggesting better liver lipid metabolic profile. On the other hand, RSG nearly had no effects on these lipids except for reducing LDL-c level, suggesting the advantage of using DA to manage blood glucose and lipid metabolism over RSG.

In the liver, DA also activated PPAR-α and its target gene which were reduced by HFD, including acyl-Coenzyme A dehydrogenase, C-4 to C-12 straight chain (ACADM; F (3, 28) = 111.1, $p < 0.0001$) and CPT1α (F (3, 28) = 177.2; $p < 0.0001$) both of which are involved in β-oxidation (Fig. 7A, B). In addition, DA, especially at a high dose, up-regulated other genes involved in the free fatty acid breakdown and β-oxidation (Fig. 7C). DA also dose-dependently decreased mRNA expression of inflammatory factors commonly involved in liver diseases and injury, *IL-1β* (F (3, 8) = 35.23, $p < 0.0001$), *IL-6* (F (3, 8) = 95.87, $p < 0.0001$), *TNF-α* (F (3, 8) = 52.07, $p < 0.0001$), *COX-1* (F (3, 8) = 45.4, $p < 0.0001$) and *COX-2* (F (3, 8) = 39.15, $p < 0.0001$) (Fig. 7D).

3.6. DA activates PPAR-γ and decreases proinflammatory genes in adipose tissue

In HFD mice, the area of white fat cells was 1.57 times bigger than that of the NCD mice, which was only reduced by DA at a high dose ($p < 0.05$ DA-H *vs.* HFD, Fig. 8A, B; F (4, 25) = 5.691, p = 0.0021). DA, especially at a high dose, upregulated mRNA expression of *PPAR-γ*, *Glut-4*, *Adipor*, *FSP27*, *ACOX-1*, *FABP4*, *Adiponectin* (Fig. 8C). DA also dose-dependently inhibited the expression of several inflammatory genes (*IL-1β*: F (4, 10) = 93.66, $p < 0.0001$; *IL-6*: F (4, 10) = 30.72, $p < 0.0001$; *TNF-α*: F (4, 10) = 108.5, $p < 0.0001$) in the white fat (Fig. 8D), which are all associated with insulin resistance. Brown adipose tissue is in charge of thermogenesis in small mammals. DA at a high dose normalized the uncoupling protein UCP-1 protein level (Fig. 8E, F; F (4, 25) = 4.97; $p < 0.01$ DA-H *vs.* HFD,), suggesting that heat production restored.

4. Discussion

Based on cell viability assays and binding assays, we found that DA is more suitable than AA for clinical translation due to its higher binding efficiency and lower toxicity (Fig. 1, Supl Fig. S1). Thus, the biological assessments only focused on DA. The major findings in this study are the direct evidence of DA binding to PPAR-α and PPAR-γ to activate both pathways (Fig. 1), and confirm its mechanism of action underlying glycemic control and lipid metabolism by using PPAR-α and PPAR-γ antagonist *in vitro* (Supl Fig. S2) and *in vivo* (Fig. 4). The superiority of DA over the classical anti-diabetic medication RSG lies in its ability to reduce blood LDL-c levels (Table 2) and hepatic steatosis (Fig. 6), increase blood HDL-c levels (Table 2), and has liver protection. The effect of DA to promote lipid metabolism may be mitochondrial driven.

PPARs play an important role in metabolic disorders, therefore have attracted significant attentions to develop/discover potent agonists. Previous studies only reported that DA could increase mRNA expression or activities of *PPAR-γ* and *PPAR-α* [23]; however, none showed how DA directly connects to these two receptors. There are many pathways to regulate PPARγ, including Axl/HSP90 [43], or ATK/mTOR [44], SIRT1 [45]. Here, the luciferase reporter gene cloning LBD fusion protein and molecular docking method were used to confirm that DA is able to form hydrogen bonds with LBD-PPAR-γ and PPAR-α, rather than non-specific bindings. These results provide evidence for suggesting that PPAR-γ and PPAR-α are the direct targets of DA (Fig. 1). The additional use of specific PPAR-γ and PPAR-α antagonists *in vitro* and *in vivo* further confirmed DA's dual-action on PPAR-γ and PPAR-α resulting in effective glycemic control and lipid lowering effects in HFD-fed mice (Supl Fig. S2, Fig. 4), respectively, which were further supported by the upregulation of the elements of the pathway for both receptors.

DA regulates glucose metabolism in the white fat, and shares similar mechanisms to the hypoglycemic effects of the 2nd line anti-diabetic drug RSG. This includes upregulating Glut-4 to facilitate the uptake of postprandial glucose surge and promoting adipocyte differentiation to receive more glucose for long-term storage. It needs to be noted that DA requires a higher dose than RSG to achieve similar effects on glycemic control, due to its lower binding efficiency with PPAR-γ than that of RSG. Nevertheless, the major discovery here is the advantage of DA

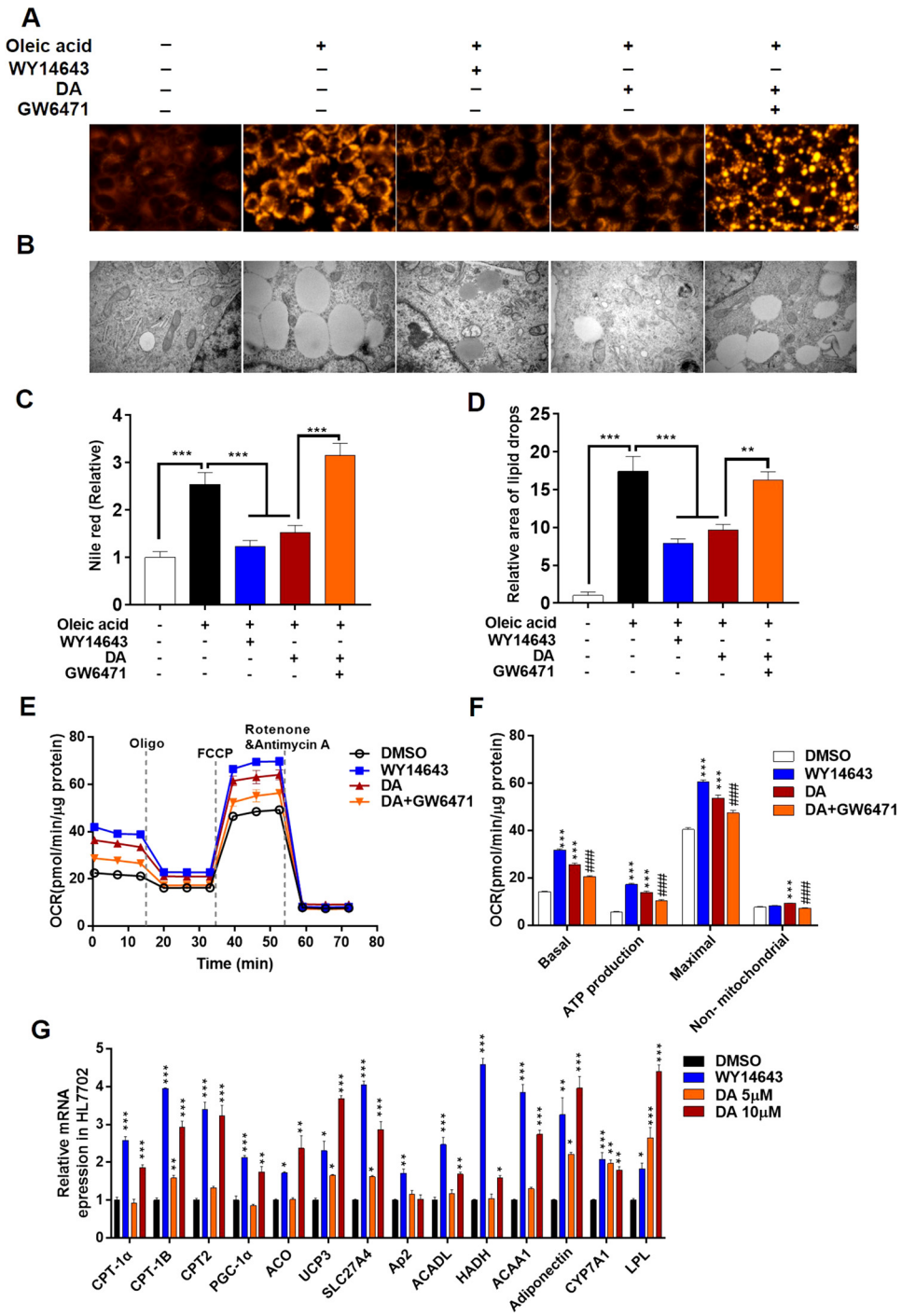

Fig. 4. DA decreases lipid accumulation in HL7702 and promotes mitochondrial oxygen consumption *via* PPAR-α. Representative images and quantifications of nile red staining (A, C) and lipid droplets by electron microscope (B, D) in HL7702 cells (n = 6). (E, F) The OCR measured by seahorse bioanalyzer in HL7702, quantification of basal respiration, ATP production and maximal respiratory capacity are shown on the graphs (n = 6). (G) Effect of DA on mRNA expression of metabolic markers, n = 3, $^{*}p < 0.05$, $^{**}p < 0.01$ and $^{***}p < 0.001$ *vs.* DMSO, $^{\#}p < 0.05$, $^{\#\#}p < 0.01$ and $^{\#\#\#}p < 0.001$ DA *vs.* DA + GW6471 group. Data are expressed as mean ± SEM. DA: Dehydroabietic acid; AA: Abietic acid; RSG: Rosiglitazone.

over RSG, due to its ability to reduce hepatic steatosis and manage blood cholesterol levels in obesity (Fig. 6, Table 2), in addition to its hypoglycemic effects. The excess fat influx from the HFD can increase circulating lipid levels leading to ectopic lipid storage in the liver leading to steatosis. This can, in turn, lead to liver metabolic dysfunction, insulin resistance and dyslipidemia. The deposition in the arteries can lead to the formation of atherosclerosis blocking blood supplies. Thus, obesity is usually associated with a series of metabolic abnormalities, resulting in high risks of cardiovascular and cerebrovascular diseases [3–5]. Diabetes itself can accelerate the development of atherosclerosis due to increasing lipid production by the liver. RSG has been taken off the shelf in the US due to the significant cardiovascular side effects, and advised to be used in patients without cardiovascular conditions in other countries [11]. However, DA could improve mitochondrial function in liver cells, while fatty acid β-oxidative is a vital process to generate ATP from the lipids in the mitochondria. This results in a better blood lipid profile and ameliorates hepatic lipid deposition albeit HFD consumption *ad libitum*, contributing to its additional activation on PPAR-α [13,46].

Another benefit of DA used in HFD-fed mice is its weight loss effect. PPAR-γ agonists can increase body weight due to both hypertrophy and hyperplasia. Although DA can promote pre-adipocyte differentiation, hypertrophy did not occur. On the contrary, fat cell size was nearly normalized to the level of the control group albeit improved glucose uptake ability. Increased thermogenesis reflected by an increase in UCP-1 expression in the brown adipose tissue may mobilize the fat storage, whereas mitochondrial β-oxidative may also increase in the adipocytes.

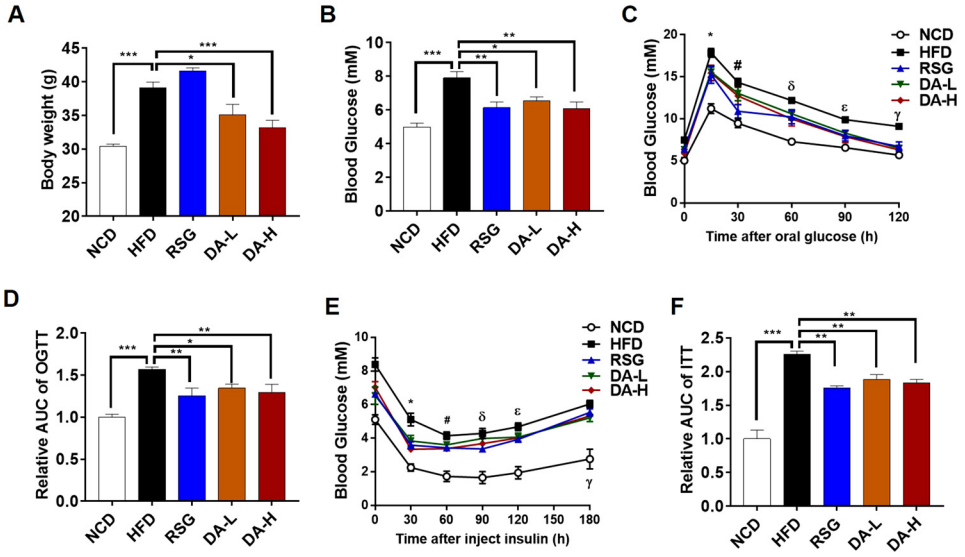

Fig. 5. DA ameliorates high fat diet-induced insulin resistance. Effect of DA treatment on body weight (A) and fasting blood glucose (B), (C) oral glucose tolerance test (OGTT; $^{*}p < 0.05$, NCD *vs.* HFD at 15 min; $^{\#}p < 0.05$, NCD and RSG *vs.* HFD at 30 min; $^{\delta}p < 0.05$, NCD and DA-H *vs.* HFD at 60 min; $^{\varepsilon}p < 0.05$, NCD and RSG and DA-H *vs.* HFD at 90 min; $^{\gamma}p < 0.05$, NCD and RSG and DA-L and DA-H *vs.* HFD at 120 min;) and the area under the curve (AUC) of OGTT in (D), insulin tolerance test (ITT, E, $^{*}p < 0.05$, NCD and RSG and DA-L and DA-H *vs.* HFD at 30 min; $^{\#}p < 0.05$, NCD *vs.* HFD at 60 min; $^{\delta}p < 0.05$, NCD and RSG *vs.* HFD at 90 min; $^{\varepsilon}p < 0.05$, NCD and *vs.* HFD at 120 min; $^{\gamma}p < 0.05$, NCD and *vs.* HFD at 120 min) and the AUC of the ITT in (F). Data are expressed as mean ± SEM, n = 6, $^{*}p < 0.05$, $^{**}p < 0.01$ and $^{***}p < 0.001$. DA-H: high dose of Dehydroabietic acid (20 mg/kg/d); DA-L: low dose of Dehydroabietic acid (10 mg/kg/d); RSG: Rosiglitazone (4 mg/kg/d).

PPAR-γ agonists (RSG and thiazolidinediones) are known for their liver toxicity which has been shown in the HFD-fed mice here, reflected by increasing liver injury enzymes ALT and AST (Fig. 6). Therefore, regular liver function surveillance is required to patients take thiazolidinediones and RSG. DA seems to overcome such side effects, showing liver protection in this study, reflected by reducing inflammation and liver injury enzymes in HFD-fed mice. The anti-inflammatory effects of DA in both white fat and liver may be still due to its activation on PPAR-α [47,48].

High fat-induced inflammation is considered to be an important pathological result of obesity, and is closely related to the increased risk of various diseases, including IR and hepatic steatosis [49]. HFD induced chronic inflammation, leading to excessive accumulation of fat in various tissues, most notably in adipose tissue, as well as other insulin-responsive organs, including the liver, which pre-disposes an individual to the development of metabolic abnormalities. PPARγ agonists inhibiting NF-κB-mediated proinflammatory cytokine expression *via* the PPARγ/PTEN pathways [31]. Evidence suggests that PPARα can counter inflammation *via* multiple, distinct mechanisms [13], including negatively regulates pro-inflammatory and acute phase response (APR) signaling pathways [50,51]. Thus, dual PPAR agonists constitute promising strategies for the treatment of T2DM. PPAR also plays the key regulatory role during the pathogenesis of inflammation induced by HFD [47,48]. There have been some reports of DA anti-inflammatory effects, such as DA reverses several cells response stimulated by TNF-α in human adult dermal fibroblasts [52]. In our research, DA improved HFD-induced inflammatory responses in liver (Fig. 7) and adipose tissue (Fig. 8), this is consistent with the effect activation of PPAR-γ and -α.

In conclusion, our work explored the potential therapeutic value of the naturally occurring compound DA. Our results suggest DA is more superior to the PPAR-γ agonist RSG for its additional beneficial effect on blood lipid management, liver steatosis and liver functional protection, especially in the setting of long-tern HFD consumption.

Funding

This work was supported by the Postdoctoral Foundation of China

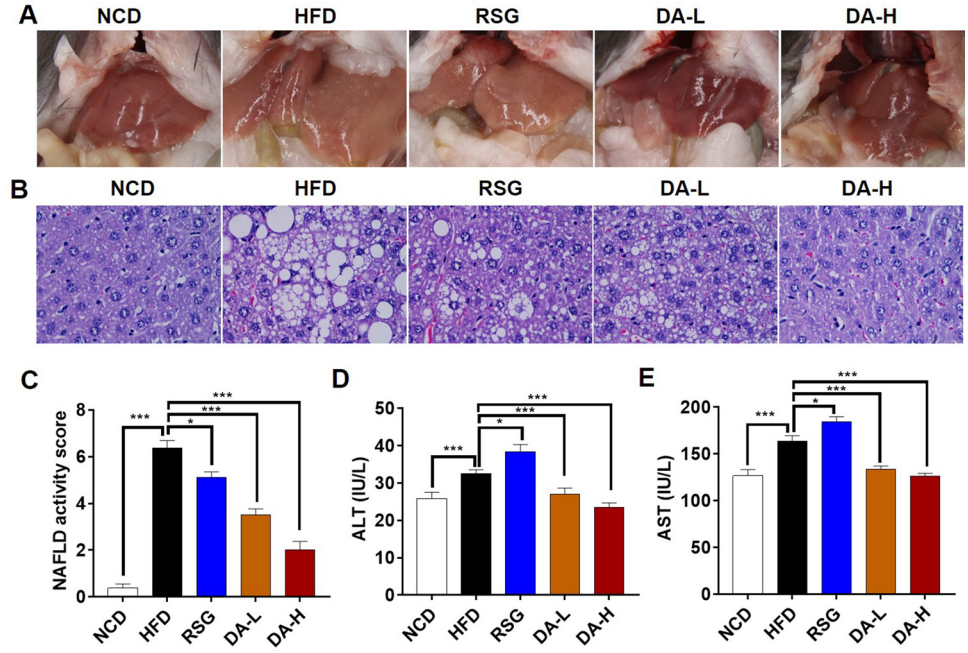

Fig. 6. DA alleviates dyslipidemia induced by high fat diet consumption in mice. (A) Representative morphology photograph of liver. (B) H&E staining of liver. (C) NAFLD activity score. ALT (D) and AST (E) levels in blood. Data are expressed as mean ± SEM, n = 6, $^{*}p < 0.05$, $^{**}p < 0.01$ and $^{***}p < 0.001$. DA-H: high dose of Dehydroabietic acid (20 mg/kg/d); DA-L: low dose of Dehydroabietic acid (10 mg/kg/d); RSG: Rosiglitazone (4 mg/kg/d).

Table 1
The nonalcoholic steatohepatitis activity score.

	NCD	HFD	RSG	DA-L	DA-H
Steatosis	0.00 ± 0.00	2.50 ± 0.19$^{###}$	2.38 ± 0.18	1.88 ± 0.23	0.88 ± 0.23***
Inflammation	0.13 ± 0.13	2.00 ± 0.27$^{###}$	1.25 ± 0.16$^{#}$	1.13 ± 0.13*	0.75 ± 0.16**
Ballooning	0.25 ± 0.16	1.88 ± 0.13$^{###}$	1.5 ± 0.19	0.50 ± 0.19***	0.38 ± 0.18***

$^{###}$p < 0.001 *vs.* NCD group, *p < 0.05, **p < 0.01 and ***p < 0.001 *vs.* HFD group.

Table 2
DA alleviated dyslipidemia induced by high fat diet consumption *in vivo*.

	NCD	HFD	RSG	DA-L	DA-H
TG	0.756 ± 0.0246	1.146 ± 0.0874$^{##}$	0.963 ± 0.101	0.803 ± 0.070**	0.765 ± 0.0533**
TC	1.783 ± 0.160	4.148 ± 0.192$^{###}$	3.708 ± 0.106	3.586 ± 0.082*	3.260 ± 0.170***
HDL-c	1.704 ± 0.086	2.368 ± 0.074$^{###}$	2.498 ± 0.114	2.885 ± 0.152***	3.182 ± 0.063***
LDL-c	0.300 ± 0.007	0.716 ± 0.046$^{###}$	0.600 ± 0.019*	0.510 ± 0.018***	0.466 ± 0.039***

$^{###}$p < 0.001 *vs.* NCD group, *p < 0.05, **p < 0.01 and ***p < 0.001 *vs.* HFD group.

(No.2018M642761); the Special Research Project of Henan Province on Traditional Chinese Medicine (No.2018ZYD12, No.2018ZY1009); and the Key Scientific Research Project Plan of Henan Higher Education Institutions (No.19A520002, No.19A360021); Central China Thousand Talents Project (No.204200510022).

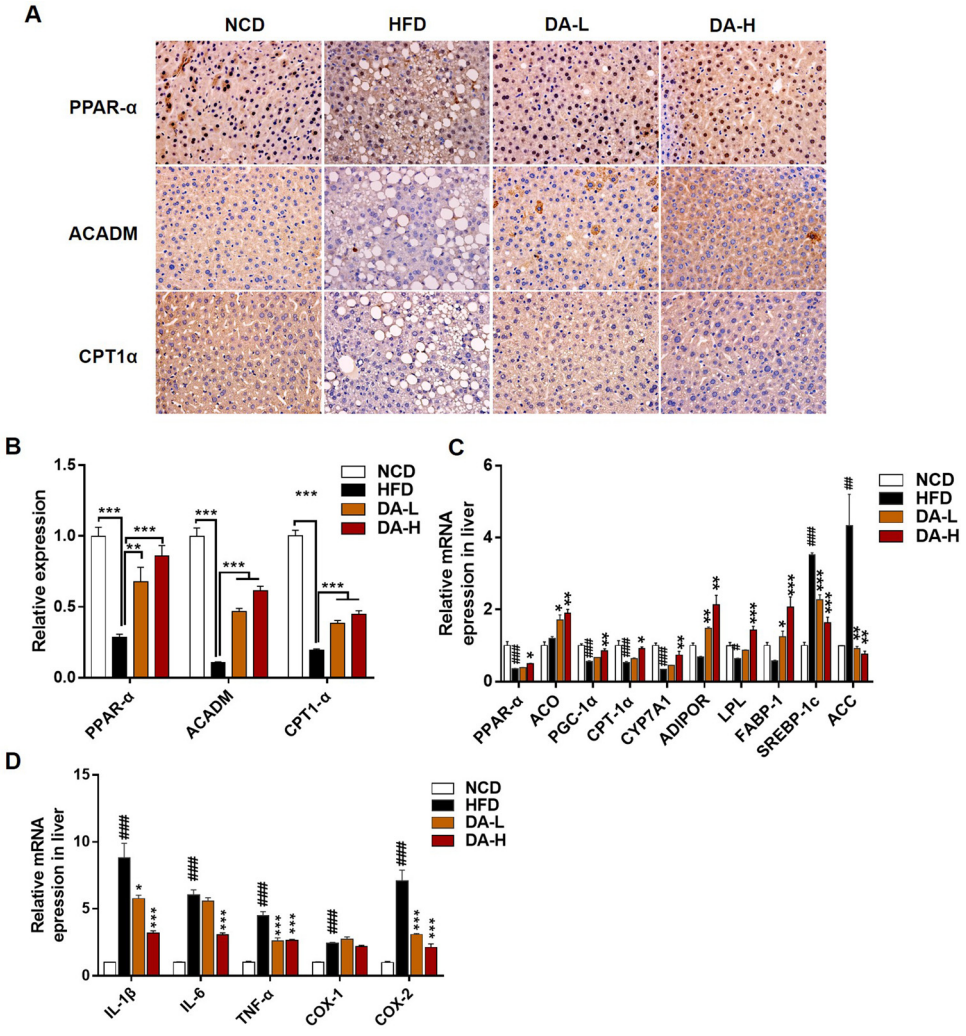

Fig. 7. DA activates PPAR-α and inhibits mRNA expression of inflammatory factors in the liver. (A) representative immunohistochemistry staining of PPAR-α, ACADM, CPT1α in the liver. (B) Quantification of the immunohistochemistry staining, n = 6. (C) mRNA expression of known PPAR-α signaling genes in the liver. (D) mRNA expression of inflammatory cytokines. Data are expressed as mean ± SEM, n = 3, *$p < 0.05$, **$p < 0.01$ and ***$p < 0.001$. DA-H: high dose of Dehydroabietic acid (20 mg/kg/d); DA-L: low dose of Dehydroabietic acid (10 mg/kg/d); RSG: Rosiglitazone (4 mg/kg/d).

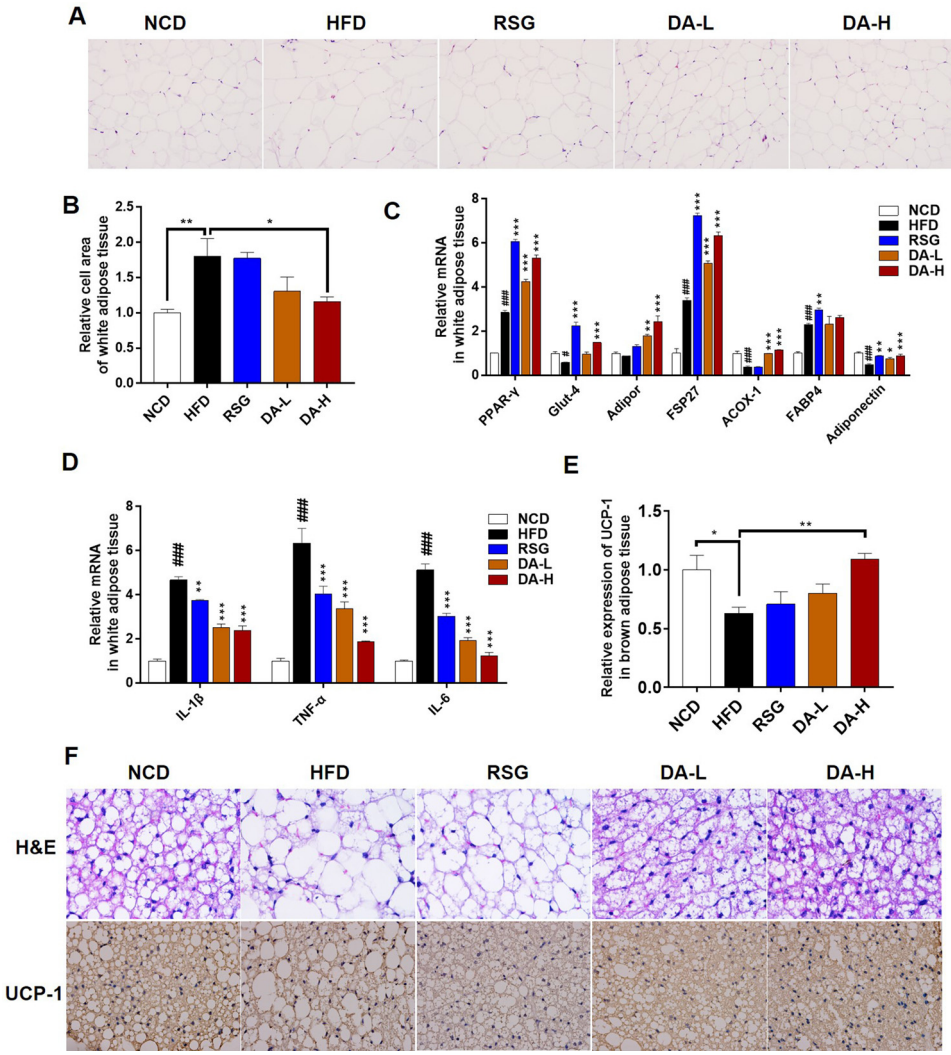

Fig. 8. DA activates PPAR-γ and decreases lipid levels in adipose tissue. (A) representative images of white adipose tissue H&E staining. (B) white fat cell area (n = 6). (C) mRNA expression of known PPAR-γ target genes in white adipose tissue (n = 3). mRNA expression of inflammatory cytokines *IL-1β*, *TNF-α*, and *IL-6* (D), (n = 3). (E, F) UCP-1 immunohistochemical analysis and representative images in the brown adipose tissue (n = 6). Data are expressed as mean ± SEM. (B, E) $^{*}p < 0.05$, $^{**}p < 0.01$ and $^{***}p < 0.001$; (C, D) $^{*}p < 0.05$, $^{**}p < 0.01$ and $^{***}p < 0.001$*vs.* HFD; $^{\#}p < 0.05$, $^{\#\#}p < 0.01$ and $^{\#\#\#}p < 0.001$ *vs.* NCD.

Contributions

Data collection, Gai Gao, Yong Yuan and Junying Song; data analysis, Yu Fu, Pan Wang, Erwen Li; experimental design, Hui Wang; project design, Zhenqiang Zhang, Jiangyan Xu; data interpretation and manuscript writing, Zhishen Xie, Hui Chen; manuscript editing, Christian Hölscher.

Declaration of Competing Interest

The authors declare no conflict of interests.

Acknowledgments

We would like to acknowledge Caili Zhang, Xianghua Liu, and Ning Sun (TEM. center, Henan University of Chinese Medicine) for their help with transmission electron microscope imaging in this study.

Appendix A. Supplementary data

Supplementary material related to this article can be found, in the online version, at doi:https://doi.org/10.1016/j.biopha.2020.110155.

References

[1] O. Tang, K. Matsushita, J. Coresh, A.R. Sharrett, J.W. McEvoy, B.G. Windham, C.M. Ballantyne, E. Selvin, Mortality implications of prediabetes and diabetes in older adults, Diabetes Care (2019).
[2] A. Ceriello, A. Nicolucci, Intensive glucose control and type 2 diabetes - 15 years on, N. Engl. J. Med. 381 (13) (2019) 1292–1293.
[3] Y. Zheng, S.H. Ley, F.B. Hu, Global aetiology and epidemiology of type 2 diabetes mellitus and its complications, Nat. Rev. Endocrinol. (2017).
[4] M. Lean, L. McCombie, J. McSorely, Trends in type 2 diabetes, BMJ 366 (2019) l5407.
[5] J. Williams, M. Loeffler, Global trends in type 2 diabetes, 2007-2017, JAMA 322 (16) (2019) 1542.
[6] V. Dubois, J. Eeckhoute, P. Lefebvre, B. Staels, Distinct but complementary contributions of PPAR isotypes to energy homeostasis, J. Clin. Invest. 127 (4) (2017) 1202–1214.
[7] B. Gross, M. Pawlak, P. Lefebvre, B. Staels, PPARs in obesity-induced T2DM, dyslipidaemia and NAFLD, Nat. Rev. Endocrinol. 13 (1) (2017) 36–49.
[8] C. Janani, B.D. Ranjitha Kumari, PPAR gamma gene–a review, Diabetes Metab. Syndr. 9 (1) (2015) 46–50.
[9] R.E. Soccio, E.R. Chen, M.A. Lazar, Thiazolidinediones and the promise of insulin sensitization in type 2 diabetes, Cell Metab. 20 (4) (2014) 573–591.
[10] B. Eliasson, U. Smith, S. Mullen, S.W. Cushman, A.S. Sherman, J. Yang, Amelioration of insulin resistance by rosiglitazone is associated with increased adipose cell size in obese type 2 diabetic patients, Adipocyte 3 (4) (2014) 314–321.
[11] M. Ahmadian, J.M. Suh, N. Hah, C. Liddle, A.R. Atkins, M. Downes, R.M. Evans, PPARgamma signaling and metabolism: the good, the bad and the future, Nat. Med. 19 (5) (2013) 557–566.
[12] F. Hong, P. Xu, Y. Zhai, The opportunities and challenges of peroxisome

proliferator-activated receptors ligands in clinical drug discovery and development, Int. J. Mol. Sci. 19 (8) (2018).
[13] N. Bougarne, B. Weyers, S.J. Desmet, J. Deckers, D.W. Ray, B. Staels, K. De Bosscher, Molecular actions of PPARalpha in lipid metabolism and inflammation, Endocr. Rev. 39 (5) (2018) 760–802.
[14] G.A. Preidis, K.H. Kim, D.D. Moore, Nutrient-sensing nuclear receptors PPARalpha and FXR control liver energy balance, J. Clin. Invest. 127 (4) (2017) 1193–1201.
[15] A. Iershov, I. Nemazanyy, C. Alkhoury, M. Girard, E. Barth, N. Cagnard, A. Montagner, D. Chretien, E.I. Rugarli, H. Guillou, M. Pende, G. Panasyuk, The class 3 PI3K coordinates autophagy and mitochondrial lipid catabolism by controlling nuclear receptor PPARalpha, Nat. Commun. 10 (1) (2019) 1566.
[16] K. Huang, M. Du, X. Tan, L. Yang, X. Li, Y. Jiang, C. Wang, F. Zhang, F. Zhu, M. Cheng, Q. Yang, L. Yu, L. Wang, D. Huang, K. Huang, PARP1-mediated PPARalpha poly(ADP-ribosyl)ation suppresses fatty acid oxidation in non-alcoholic fatty liver disease, J. Hepatol. 66 (5) (2017) 962–977.
[17] N. Jain, S. Bhansali, A.V. Kurpad, M. Hawkins, A. Sharma, S. Kaur, A. Rastogi, A. Bhansali, Effect of a dual PPAR alpha/gamma agonist on insulin sensitivity in patients of type 2 diabetes with hypertriglyceridemia- randomized double-blind placebo-controlled trial, Sci. Rep. 9 (1) (2019) 19017.
[18] Z. Ament, J.A. West, E. Stanley, T. Ashmore, L.D. Roberts, J. Wright, A.W. Nicholls, J.L. Griffin, PPAR-pan activation induces hepatic oxidative stress and lipidomic remodelling, Free Radic. Biol. Med. 95 (2016) 357–368.
[19] U. Kaul, D. Parmar, K. Manjunath, M. Shah, K. Parmar, K.P. Patil, A. Jaiswal, New dual peroxisome proliferator activated receptor agonist-Saroglitazar in diabetic dyslipidemia and non-alcoholic fatty liver disease: integrated analysis of the real world evidence, Cardiovasc. Diabetol. 18 (1) (2019) 80.
[20] M.D. Goncalves, B.T.S. Bortoleti, F. Tomiotto-Pellissier, M.M. Miranda-Sapla, J.P. Assolini, A.C.M. Carloto, P.G.C. Carvalho, E.T. Tudisco, A. Urbano, S.R. Ambrosio, E.Y. Hirooka, A.N.C. Simao, I.N. Costa, W.R. Pavanelli, I. Conchon-Costa, N.S. Arakawa, Dehydroabietic acid isolated from Pinus elliottii exerts in vitro antileishmanial action by pro-oxidant effect, inducing ROS production in promastigote and downregulating Nrf2/ferritin expression in amastigote forms of Leishmania amazonensis, Fitoterapia 128 (2018) 224–232.
[21] Y. Zhu, S. Zhang, Z. Geng, D. Wang, F. Liu, M. Zhang, H. Bian, W. Xu, Analysis of abietic acid and dehydroabietic acid residues in raw ducks and cooked ducks, Poult. Sci. 93 (10) (2014) 2663–2667.
[22] J. Kim, Y.G. Kang, J.Y. Lee, D.H. Choi, Y.U. Cho, J.M. Shin, J.S. Park, J.H. Lee, W.G. Kim, D.B. Seo, T.R. Lee, Y. Miyamoto, K.T. No, The natural phytochemical dehydroabietic acid is an anti-aging reagent that mediates the direct activation of SIRT1, Mol. Cell. Endocrinol. 412 (2015) 216–225.
[23] M.S. Kang, S. Hirai, T. Goto, K. Kuroyanagi, J.Y. Lee, T. Uemura, Y. Ezaki, N. Takahashi, T. Kawada, Dehydroabietic acid, a phytochemical, acts as ligand for PPARs in macrophages and adipocytes to regulate inflammation, Biochem. Biophys. Res. Commun. 369 (2) (2008) 333–338.
[24] E. Kim, Y.G. Kang, Y.J. Kim, T.R. Lee, B.C. Yoo, M. Jo, J.H. Kim, J.H. Kim, D. Kim, J.Y. Cho, Dehydroabietic acid suppresses inflammatory response via suppression of Src-, Syk-, and TAK1-mediated pathways, Int. J. Mol. Sci. 20 (7) (2019).
[25] W.S. Li, J.D. McChesney, Preparation of potential anti-inflammatory agents from dehydroabietic acid, J. Pharm. Sci. 81 (7) (1992) 646–651.
[26] L.F. Leandro, M.J. Cardoso, S.D. Silva, M.G. Souza, R.C. Veneziani, S.R. Ambrosio, C.H. Martins, Antibacterial activity of Pinus elliottii and its major compound, dehydroabietic acid, against multidrug-resistant strains, J. Med. Microbiol. 63 (Pt 12) (2014) 1649–1653.
[27] X. Wang, F.H. Pang, L. Huang, X.P. Yang, X.L. Ma, C.N. Jiang, F.Y. Li, F.H. Lei, Synthesis and biological evaluation of novel dehydroabietic acid-oxazolidinone hybrids for antitumor properties, Int. J. Mol. Sci. 19 (10) (2018).
[28] D. Luo, Q. Ni, A. Ji, W. Gu, J. Wu, C. Jiang, Dehydroabietic acid derivative QC4 induces gastric cancer cell death via oncosis and apoptosis, Biomed Res. Int. 2016 (2016) 2581061.
[29] M.S. Kang, S. Hirai, T. Goto, K. Kuroyanagi, Y.I. Kim, K. Ohyama, T. Uemura, J.Y. Lee, T. Sakamoto, Y. Ezaki, R. Yu, N. Takahashi, T. Kawada, Dehydroabietic acid, a diterpene, improves diabetes and hyperlipidemia in obese diabetic KK-Ay mice, Biofactors 35 (5) (2009) 442–448.
[30] N. Takahashi, R. Yao, M.S. Kang, M. Senda, C. Ando, K. Nishimura, T. Goto, S. Hirai, Y. Ezaki, T. Kawada, Dehydroabietic acid activates peroxisome proliferator-activated receptor-gamma and stimulates insulin-dependent glucose uptake into 3T3-L1 adipocytes, Biofactors 37 (4) (2011) 309–314.
[31] Z.F. Wang, J. Li, C. Ma, C. Huang, Z.Q. Li, Telmisartan ameliorates Abeta oligomer-induced inflammation via PPARgamma/PTEN pathway in BV2 microglial cells, Biochem. Pharmacol. 171 (2020) 113674.
[32] C. Huang, Y. Zhang, Z. Gong, X. Sheng, Z. Li, W. Zhang, Y. Qin, Berberine inhibits 3T3-L1 adipocyte differentiation through the PPARgamma pathway, Biochem. Biophys. Res. Commun. 348 (2) (2006) 571–578.
[33] Z. Xie, J. Zhao, H. Wang, Y. Jiang, Q. Yang, Y. Fu, H. Zeng, C. Holscher, J. Xu, Z. Zhang, Magnolol alleviates Alzheimer's disease-like pathology in transgenic C. elegans by promoting microglia phagocytosis and the degradation of beta-amyloid through activation of PPAR-gamma, Biomed. Pharmacother. 124 (2020) 109886.
[34] L. Feng, H. Luo, Z. Xu, Z. Yang, G. Du, Y. Zhang, L. Yu, K. Hu, W. Zhu, Q. Tong, K. Chen, F. Guo, C. Huang, Y. Li, Bavachinin, as a novel natural pan-PPAR agonist, exhibits unique synergistic effects with synthetic PPAR-gamma and PPAR-alpha agonists on carbohydrate and lipid metabolism in db/db and diet-induced obese mice, Diabetologia 59 (6) (2016) 1276–1286.
[35] S.X. Meng, Q. Liu, Y.J. Tang, W.J. Wang, Q.S. Zheng, H.J. Tian, D.S. Yao, L. Liu, J.H. Peng, Y. Zhao, Y.Y. Hu, Q. Feng, A recipe composed of chinese herbal active components regulates hepatic lipid metabolism of NAFLD in vivo and in vitro, Biomed Res. Int. 2016 (2016) 1026852.
[36] Z. Xie, T. Loi Truong, P. Zhang, F. Xu, X. Xu, P. Li, Dan-Qi prescription ameliorates insulin resistance through overall corrective regulation of glucose and fat metabolism, J. Ethnopharmacol. 172 (2015) 70–79.
[37] X. Yang, Y. Fu, F. Hu, X. Luo, J. Hu, G. Wang, PIK3R3 regulates PPARalpha expression to stimulate fatty acid beta-oxidation and decrease hepatosteatosis, Exp. Mol. Med. 50 (1) (2018) e431.
[38] S. Terzo, G.F. Caldara, V. Ferrantelli, R. Puleio, G. Cassata, F. Mule, A. Amato, Pistachio consumption prevents and improves lipid dysmetabolism by reducing the lipid metabolizing gene expression in diet-induced obese mice, Nutrients 10 (12) (2018).
[39] A.R.R. Vicentino, V.C. Carneiro, D. Allonso, R.F. Guilherme, C.F. Benjamim, H.A.M. Dos Santos, F. Xavier, A.D.S. Pyrrho, J.A.S. Gomes, M.C. Fonseca, R.C. de Oliveira, T.A. Pereira, L. Ladislau, J.R. Lambertucci, M.R. Fantappie, Emerging role of HMGB1 in the pathogenesis of schistosomiasis liver fibrosis, Front. Immunol. 9 (2018) 1979.
[40] E.M. Brunt, D.E. Kleiner, L.A. Wilson, P. Belt, B.A. Neuschwander-Tetri, Nonalcoholic fatty liver disease (NAFLD) activity score and the histopathologic diagnosis in NAFLD: distinct clinicopathologic meanings, Hepatology 53 (3) (2011) 810–820.
[41] Y.L. Chen, W. Xu, R.H. Rosa Jr., L. Kuo, T.W. Hein, Hyperglycemia enhances constriction of retinal venules via activation of the reverse-mode sodium-calcium exchanger, Diabetes 68 (8) (2019) 1624–1634.
[42] S.Y. Jiang, H. Li, J.J. Tang, J. Wang, J. Luo, B. Liu, J.K. Wang, X.J. Shi, H.W. Cui, J. Tang, F. Yang, W. Qi, W.W. Qiu, B.L. Song, Discovery of a potent HMG-CoA reductase degrader that eliminates statin-induced reductase accumulation and lowers cholesterol, Nat. Commun. 9 (1) (2018) 5138.
[43] M. Zhang, C. Qian, Z.G. Zheng, F. Qian, Y. Wang, P.M. Thu, X. Zhang, Y. Zhou, L. Tu, Q. Liu, H.J. Li, H. Yang, P. Li, X. Xu, Jujuboside A promotes Abeta clearance and ameliorates cognitive deficiency in Alzheimer's disease through activating Axl/HSP90/PPARgamma pathway, Theranostics 8 (15) (2018) 4262–4278.
[44] H. Sun, X. Zhu, W. Cai, L. Qiu, Hypaphorine attenuates lipopolysaccharide-induced endothelial inflammation via regulation of TLR4 and PPAR-gamma dependent on PI3K/Akt/mTOR signal pathway, Int. J. Mol. Sci. 18 (4) (2017).
[45] R. Wang, J.J. Li, S. Diao, Y.D. Kwak, L. Liu, L. Zhi, H. Bueler, N.R. Bhat, R.W. Williams, E.A. Park, F.F. Liao, Metabolic stress modulates Alzheimer's beta-secretase gene transcription via SIRT1-PPARgamma-PGC-1 in neurons, Cell Metab. 17 (5) (2013) 685–694.
[46] N. Liang, A. Damdimopoulos, S. Goni, Z. Huang, L.L. Vedin, T. Jakobsson, M. Giudici, O. Ahmed, M. Pedrelli, S. Barilla, F. Alzaid, A. Mendoza, T. Schroder, R. Kuiper, P. Parini, A. Hollenberg, P. Lefebvre, S. Francque, L. Van Gaal, B. Staels, N. Venteclef, E. Treuter, R. Fan, Hepatocyte-specific loss of GPS2 in mice reduces non-alcoholic steatohepatitis via activation of PPARalpha, Nat. Commun. 10 (1) (2019) 1684.
[47] S. Choi, J.E. Jung, Y.R. Yang, E.S. Kim, H.J. Jang, E.K. Kim, I.S. Kim, J.Y. Lee, J.K. Kim, J.K. Seo, J.M. Kim, J. Park, P.G. Suh, J.H. Choi, Novel phosphorylation of PPARgamma ameliorates obesity-induced adipose tissue inflammation and improves insulin sensitivity, Cell. Signal. 27 (12) (2015) 2488–2495.
[48] Y. Hou, F. Moreau, K. Chadee, PPARgamma is an E3 ligase that induces the degradation of NFkappaB/p65, Nat. Commun. 3 (2012) 1300.
[49] J.M. Olefsky, C.K. Glass, Macrophages, inflammation, and insulin resistance, Annu. Rev. Physiol. 72 (2010) 219–246.
[50] M. Pawlak, P. Lefebvre, B. Staels, Molecular mechanism of PPARalpha action and its impact on lipid metabolism, inflammation and fibrosis in non-alcoholic fatty liver disease, J. Hepatol. 62 (3) (2015) 720–733.
[51] B. Wu, X. Sun, B. Yuan, F. Ge, H.B. Gupta, H.C. Chiang, J. Li, Y. Hu, T.J. Curiel, R. Li, PPARγ inhibition boosts efficacy of PD-L1 Checkpoint Blockade Immunotherapy against Murine Melanoma in a sexually dimorphic manner, Int. J. Biol. Sci. 16 (9) (2020) 1526–1535.
[52] X.W. Wang, Y. Yu, L. Gu, Dehydroabietic acid reverses TNF-alpha-induced the activation of FOXO1 and suppression of TGF-beta1/Smad signaling in human adult dermal fibroblasts, Int. J. Clin. Exp. Pathol. 7 (12) (2014) 8616–8626.